Carbon Nanotubes—the Route Toward Applications

Ray H. Baughman,[1,2]* Anvar A. Zakhidov,[1,3] Walt A. de Heer[4]

Many potential applications have been proposed for carbon nanotubes, including conductive and high-strength composites; energy storage and energy conversion devices; sensors; field emission displays and radiation sources; hydrogen storage media; and nanometer-sized semiconductor devices, probes, and interconnects. Some of these applications are now realized in products. Others are demonstrated in early to advanced devices, and one, hydrogen storage, is clouded by controversy. Nanotube cost, polydispersity in nanotube type, and limitations in processing and assembly methods are important barriers for some applications of single-walled nanotubes.

There are two main types of carbon nanotubes that can have high structural perfection. Single-walled nanotubes (SWNTs) consist of a single graphite sheet seamlessly wrapped into a cylindrical tube (Fig. 1, A to D). Multiwalled nanotubes (MWNTs) comprise an array of such nanotubes that are concentrically nested like rings of a tree trunk (Fig. 1E).

Despite structural similarity to a single sheet of graphite, which is a semiconductor with zero band gap, SWNTs may be either metallic or semiconducting, depending on the sheet direction about which the graphite sheet is rolled to form a nanotube cylinder. This direction in the graphite sheet plane and the nanotube diameter are obtainable from a pair of integers (n, m) that denote the nanotube type (*1*). Depending on the appearance of a belt of carbon bonds around the nanotube diameter, the nanotube is either of the armchair ($n = m$), zigzag ($n = 0$ or $m = 0$), or chiral (any other n and m) variety. All armchair SWNTs are metals; those with $n - m = 3k$, where k is a nonzero integer, are semiconductors with a tiny band gap; and all others are semiconductors with a band gap that inversely depends on the nanotube diameter (*1*).

The electronic properties of perfect MWNTs are rather similar to those of perfect SWNTs, because the coupling between the cylinders is weak in MWNTs. Because of the nearly one-dimensional electronic structure, electronic transport in metallic SWNTs and MWNTs occurs ballistically (i.e., without scattering) over long nanotube lengths, enabling them to carry high currents with essentially no heating (*2*, *3*). Phonons also propagate easily along the nanotube: The measured room temperature thermal conductivity for an individual MWNT (>3000 W/m·K) is greater than that of natural diamond and the basal plane of graphite (both 2000 W/m·K) (*4*). Superconductivity has also been observed, but only at low temperatures, with transition temperatures of ~0.55 K for 1.4-nm-diameter SWNTs (*5*) and ~5 K for 0.5-nm-diameter SWNTs grown in zeolites (*6*).

Small-diameter SWNTs are quite stiff and exceptionally strong, meaning that they have a high Young's modulus and high tensile strength. Literature reports of these mechanical parameters can be confusing, because some authors use the total occupied cross-sectional area and others use the much smaller van der Waals area for defining Young's modulus and tensile strength. With the total area per nanotube in a nanotube bundle for normalizing the applied force to obtain the applied stress, the calculated Young's modulus for an individual (10, 10) nanotube is ~0.64 TPa (*7*), which is consistent with measurements (*8*). Because small-diameter nanotube ropes have been extended elastically by ~5.8% before breaking, the SWNT strength calculated from the product of this strain and modulus is ~37 GPa (*8*, *9*), which is close to the maximum strength of silicon carbide nanorods (~53 GPa) (*10*). This modulus of ~0.64 TPa is about the same as that of silicon carbide nanofibers (~0.66 TPa) but lower than that of highly oriented pyrolytic graphite (~1.06 TPa) (*10*). More impressive and important for applications needing light structural materials, the density-normalized modulus and strength of this typical SWNT are, respectively, ~19 and ~56 times that of steel wire and, respectively, ~2.4 and ~1.7 times that of silicon carbide nanorods (*10*). The challenge is to achieve these properties of individual SWNTs in nanotube assemblies found in sheets and continuous fibers.

Nanotube Synthesis and Processing

SWNTs and MWNTs are usually made by carbon-arc discharge, laser ablation of carbon, or chemical vapor deposition (typically on catalytic particles) (*11*). Nanotube diameters range from ~0.4 to >3 nm for SWNTs and from ~1.4 to at least 100 nm for MWNTs (*6*, *11*). Nanotube properties can thus be tuned by changing the diameter. Unfortunately, SWNTs are presently produced only on a small scale and are extremely expensive: High-purity samples cost about $750/g, and samples containing substantial amounts of impurities cost about $60/g (*12*). Many researchers have depended on production facilities started by Rick Smalley of Rice University for purified SWNTs, on laser ablation–produced nanotubes, and now on the high-pressure carbon monoxide (HiPco) nanotubes of Carbon Nanotechnology, Inc. (CNI). CNI "hopes to make around 9 kilograms a day by 2002, and could be turning out thousands of kilograms per week by 2004" (*13*, p. 144); it is hoped that this will bring the price down.

All currently known synthesis methods for SWNTs result in major concentrations of impurities. Carbon-coated metal catalyst contaminates the nanotubes of the HiPco route, and both carbon-coated metal catalyst and, typically, ~60% forms of carbon other than nanotubes are formed in the carbon-arc route (*11*). These impurities are typically removed by acid treatment, which introduces other impurities, can degrade nanotube length and perfection, and adds to nanotube cost. Another problem, especially for electronic devices, is that the usual synthetic routes result in mixtures of various semiconducting and metallic nanotubes. Metallic SWNTs can be selectively destroyed by electrical heating, so that only the semiconducting nanotubes needed for nanotube field-effect transistors (NTFETs) survive (*14*). However, no route to substantial quantities of SWNTs of one type is yet known.

Commercial access to MWNTs is less problematic. Hyperion Catalysis International, Inc., pioneered the production of MWNTs in multiton quantities in the early 1990s.

[1]NanoTech Institute, [2]Department of Chemistry, [3]Department of Physics, University of Texas at Dallas, Richardson, TX 75083–0688, USA. [4]Department of Physics, Georgia Institute of Technology, Atlanta, GA 30332, USA.

*To whom correspondence should be addressed. E-mail: ray.baughman@utdallas.edu

However, these nanotubes have not been widely available to and used by researchers, because Hyperion has generally sold nanotubes compounded as a minority component in plastics and has traditionally required purchaser agreements that restrict the independent pursuit of patents by customers. Furthermore, MWNTs produced catalytically by gas-phase pyrolysis, like the Hyperion nanotubes, have high defect densities compared to those produced by the more expensive carbon-arc process (*11*). However, the catalytically produced tubes are adequate for many applications, especially because they can be directly synthesized without major contamination by carbonaceous impurities.

When Hyperion's extremely strong composition-of-matter patent coverage on MWNTs (*15*) expires (in 2004 in the United States), other large-scale producers of MWNTs are likely to emerge. Mitsui recently announced plans to build a $15.2 million production facility in Japan that will be capable of producing 120 ton/year (*16*). The company plans to market 20-nm-diameter MWNTs at about $75/kg.

Nanotube sheets, fibers, and composites should retain the properties of the individual nanotubes as far as possible. A generic problem is that impurities readily coat the surface of nanotubes (as do gases such as oxygen) (*17*). Even nanometer-thick coatings can affect nanotube dispersibility, binding in composites, and the electronic and mechanical properties of junctions between nanotubes. Also, SWNTs normally form bundles of parallel tubes (Fig. 1F) (*18*), such that the full surface area of the individual nanotubes is not usually available for stress transfer with the matrix. Nanotube sheets (called "nanotube paper" or "bucky paper") are conventionally obtained by filtering SWNTs dispersed in a liquid, peeling the resulting sheet from the filter after washing and drying, and annealing the sheet at high temperatures to remove impurities (*19*). If SWNTs were not so expensive and if there were a commercial need, one could make nanotube sheets with similar methods (and at a similar scale) to those used to make ordinary paper. However, the maximum Young's modulus of sheets made by the filtration process does not substantially exceed that of sheets of ordinary organic polymers (typically ~1 to 4 GPa), and it increases from ~0.3 to ~6 GPa as increasing care is taken in removing secondary impurities ("bucky goo") introduced during purification (*20*).

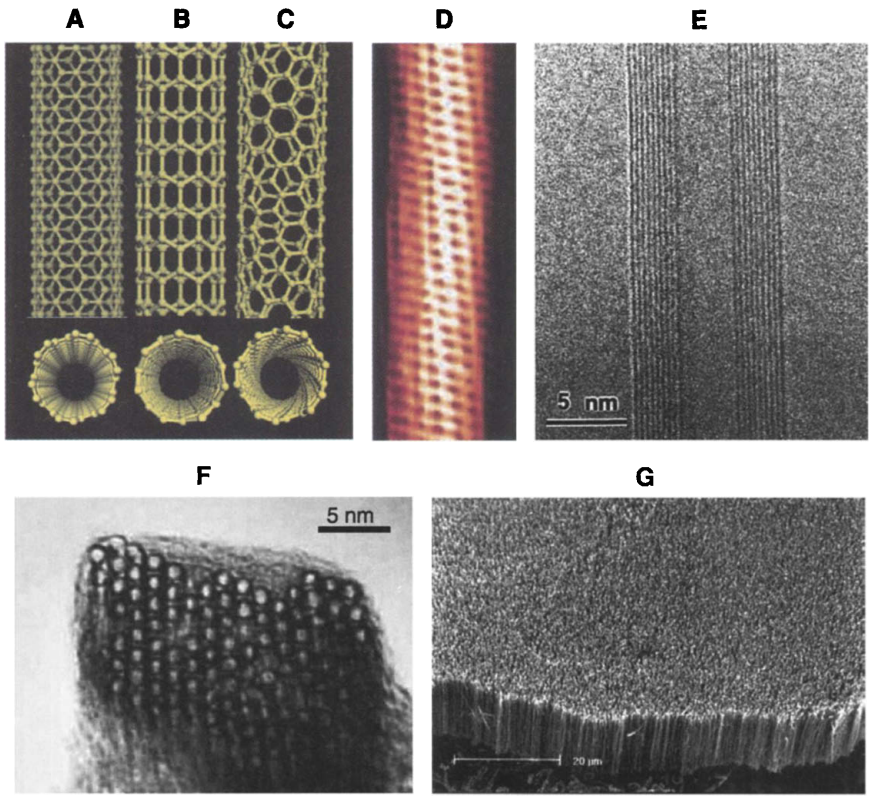

Fig. 1. Schematic illustrations of the structures of (**A**) armchair, (**B**) zigzag, and (**C**) chiral SWNTs. Projections normal to the tube axis and perspective views along the tube axis are on the top and bottom, respectively. (**D**) Tunneling electron microscope image (*72*) showing the helical structure of a 1.3-nm-diameter chiral SWNT. (**E**) Transmission electron microscope (TEM) image of a MWNT containing a concentrically nested array of nine SWNTs. (**F**) TEM micrograph (*18*) showing the lateral packing of 1.4-nm-diameter SWNTs in a bundle. (**G**) Scanning electron microscope (SEM) image of an array of MWNTs grown as a nanotube forest (micrograph courtesy of L. Dai).

Advances have been made in producing polymer-containing SWNTs by melt spinning and in aligning the nanotubes by drawing. However, the melt viscosity becomes too high for conventional melt spinning when the nanotube content is much more than 10%, and demonstrated increases in strength and modulus are much smaller than those predicted from the rule of mixtures (*21*). Vigolo and others have developed a coagulation-based process that enables them to spin continuous fibers containing mostly SWNTs (*22*, *23*). Currently, however, the draw rate from the coagulation bath is slow, the nanotube loading in the spinning solution is low (~0.4 weight %), and the nanotubes are not well aligned. The highest modulus obtained for fibers spun by a modification of Vigolo and others' coagulation-based process is ~50 GPa (*20*, *22*), more than an order of magnitude lower than the intrinsic modulus of individual SWNTs. Trace poly(vinyl alcohol) from the coagulation solution binds the nanotubes together in air more effectively than do van der Waals interactions, and it causes fiber swelling and corresponding degradation of mechanical properties in aqueous electrolytes; its removal by pyrolysis decreases Young's modulus to ~15 GPa. Creep is also a major problem for these spun fibers (*20*). A recently developed fiber-spinning method for SWNTs, which appears to involve a lyotropic liquid crystal phase, increases the nanotube concentration in the spinning solution by more than an order of magnitude and yields oriented nanotube fibers (*24*). An improvement in coupling between nanotubes appears necessary to optimize the Young's modulus and tensile strength of these spun nanotube fibers, which are presently low.

Technologies for patterned deposition of nanotubes on the micro- to nanometer scale are important for electronic devices, displays, and nanoscale actuators. With selected area deposition of catalyst, nanotubes have been grown as forests of vertically aligned MWNTs (*25*) (Fig. 1G), nanoprobes (*26*), and structures for field emission displays (*27*, *28*). By combining surface-patterning techniques with fluidic assembly methods, Huang and co-workers (*29*) have made networks of crossed nanowire arrays that are individually addressable at each junction.

Carbon Nanotube Composites

The first realized major commercial application of MWNTs is their use as electrically conducting components in polymer composites. Depending on the polymer matrix, conductivities of 0.01 to 0.1 S/cm can be obtained for 5% loading; much lower conductivity levels suffice for dissipating electrostatic charge (*30*). The low loading levels and the nanofiber morphology of the MWNTs allow electronic conductivity to be achieved while

avoiding or minimizing degradation of other performance aspects, such as mechanical properties and the low melt flow viscosity needed for thin-wall molding applications. In commercial automotive gas lines and filters, the nanotube filler dissipates charge buildup that can lead to explosions and better maintains barrier properties against fuel diffusion than do plastics filled with carbon black. Plastic semiconductor chip carriers and reading heads made from nanotube composites avoid contamination associated with carbon black sloughing. Similar materials are also used for conductive plastic automotive parts, such as mirror housings that are electrostatically painted on the assembly line, thereby avoiding separate painting and associated color mismatch. The smoothness of the surface finish provides an advantage over other conductive fillers.

Hyperion worked with major plastic producers, plastic compounders, and automotive manufacturers to develop these applications, which presently consume substantial tonnage of nanotubes. Cost dictates the use of MWNTs rather than SWNTs, but unbundled SWNTs should enable lower percolation levels, reducing the required loading levels further. A percolation threshold of 0.1 to 0.2% has been reported for SWNTs in epoxy, one-tenth that of commercially available 200-nm-diameter vapor-grown carbon fibers (*31*). The shielding of electromagnetic radiation from cell phones and computers by using molded SWNT and MWNT composites is also a potentially lucrative application, for which Eikos, Inc., has important patent coverage (*32*).

Incorporation of nanotubes into plastics can potentially provide structural materials with dramatically increased modulus and strength. The critical challenges lie in uniformly dispersing the nanotubes, achieving nanotube-matrix adhesion that provides effective stress transfer, and avoiding intratube sliding between concentric tubes within MWNTs and intrabundle sliding within SWNT ropes. Some promising results have been reported; for example, Biercuk and others (*31*) observed a monotonic increase of resistance to indentation (Vickers hardness) by up to 3.5 times on loading up to 2% SWNTs and a doubling of thermal conductivity with 1% SWNTs. Also, 1% MWNT loading in polystyrene increases the modulus and breaking stress by up to 42 and 25%, respectively (*33*).

Electrochemical Devices

Because of the high electrochemically accessible surface area of porous nanotube arrays, combined with their high electronic conductivity and useful mechanical properties, these materials are attractive as electrodes for devices that use electrochemical double-layer charge injection. Examples include "supercapacitors," which have giant capacitances in comparison with those of ordinary dielectric-based capacitors, and electromechanical actuators that may eventually be used in robots. Like ordinary capacitors, carbon nanotube supercapacitors (*34–36*) and electromechanical actuators (*37*) typically comprise two electrodes separated by an electronically insulating material, which is ionically conducting in electrochemical devices. The capacitance for an ordinary planar sheet capacitor inversely depends on the interelectrode separation. In contrast, the capacitance for an electrochemical device depends on the separation between the charge on the electrode and the countercharge in the electrolyte. Because this separation is about a nanometer for nanotubes in electrodes, as compared with the micrometer or larger separations in ordinary dielectric capacitors, very large capacitances result from the high nanotube surface area accessible to the electrolyte. These capacitances (typically between ~15 and ~200 F/g, depending on the surface area of the nanotube array) result in large amounts of charge injection when only a few volts are applied (*34–37*). This charge injection is used for energy storage in nanotube supercapacitors and to provide electrode expansions and contractions that can do mechanical work in electromechanical actuators.

Supercapacitors with carbon nanotube electrodes can be used for applications that require much higher power capabilities than batteries and much higher storage capacities than ordinary capacitors, such as hybrid electric vehicles that can provide rapid acceleration and store braking energy electrically. The capacitances (180 and 102 F/g for SWNT and MWNT electrodes, respectively) and power densities (20 kW/kg at energy densities of ~7 W·hour/kg for SWNT electrodes) (*34*, *35*) are attractive, especially because performance can likely be improved by replacing SWNT bundles and MWNTs with unbundled SWNTs. An extraordinarily short discharge time of 7 ms was reported (*36*) for 10 MWNT capacitors connected in series, which operated at up to 10 V.

Nanotube electromechanical actuators function at a few volts, compared with the ~100 V used for piezoelectric stacks and the ≥1000 V used for electrostrictive actuators. Nanotube actuators have been operated at temperatures up to 350°C, and operation above 1000°C should be possible, on the basis of SWNT thermal stability and industrial carbon electrode electrochemical application above this temperature (*20*). From observed nanotube actuator strains that can exceed 1%, order-of-magnitude advantages over commercial actuators in work per cycle and stress generation capabilities are predicted if the mechanical properties of nanotube sheets can be increased to close to the inherent mechanical properties of the individual nanotubes (*20*). The maximum observed isometric actuator stress of SWNT actuators is presently 26 MPa (*20*). This is >10 times the stress initially reported for these actuators and ~100 times that of the stress generation capability of natural muscle, and it approaches the stress generation capability of high-modulus commercial ferroelectrics (~40 MPa). However, the ability to generate stress is still >100 times lower than that predicted for nanotube fibers with the modulus of the individual SWNTs.

The achievable actuator strain is largely independent of applied load, and hence the work during isobaric (constant load) contraction linearly increases with load until the material fails. The product of actuator strain and fracture stress for nanotube actuators, normalized to density, is already 50 times the corresponding gravimetric work achieved for commercial high-modulus ferroelectrics (*20*). However, creep prohibits the application of stresses approaching the fracture stress. The success of actuator technology based on carbon nanotubes will depend on improvements in the mechanical properties of nanotube sheets and fibers with a high surface area by increasing nanotube alignment and the binding between nanotubes. Because nanotube actuation depends on ion diffusion, ferroelectrics can be cycled much faster at maximum work per cycle than can large nanotube actuators, which eliminates some applications.

The use of nanotubes as electrodes in lithium batteries is a possibility because of the high reversible component of storage capacity at high discharge rates. The maximum reported reversible capacity is 1000 mA·hour/g for SWNTs that are mechanically milled in order to enable the filling of nanotube cores, as compared to 372 mA·hour/g for graphite (*38*) and 708 mA·hour/g for ball-milled graphite (*39*). However, the large irreversible component to capacity (coexisting with the large reversible storage capacity), an absence of a voltage plateau during discharge, and the large hysteresis in voltage between charge and discharge (*38*) currently limit energy storage density and energy efficiency, as compared with those of other competing materials.

Hydrogen Storage

Nanotubes have been long heralded as potentially useful for hydrogen storage (for example, for fuel cells that power electric vehicles or laptop computers). However, experimental reports of high storage capacities are so controversial that it is impossible to assess the applications potential (*40–44*). Numerous claims of high hydrogen storage levels have been shown to be incorrect; other reports (*45*, *46*) of room temperature capacities above 6.5 weight % (a U.S. Department of Energy

benchmark) await confirmation. Given the high research activity in this area, it is hoped that this controversy will soon be resolved.

Field Emission Devices

Industrial and academic research activity on electronic devices has focused principally on using SWNTs and MWNTs as field emission electron sources (*47*, *48*) for flat panel displays (*49*), lamps (*50*), gas discharge tubes providing surge protection (*51*), and x-ray (*52*) and microwave generators (*53*). A potential applied between a carbon nanotube–coated surface and an anode produces high local fields, as a result of the small radius of the nanofiber tip and the length of the nanofiber. These local fields cause electrons to tunnel from the nanotube tip into the vacuum. Electric fields direct the field-emitted electrons toward the anode, where a phosphor produces light for the flat panel display application (Fig. 2). However, the complete picture is not nearly so simple. Unlike for ordinary bulk metals, nanotube tip electron emission arises from discrete energy states, rather than continuous electronic bands (*54*). Also, the emission behavior depends critically on the nanotube tip structure: Enhanced emission results from opening SWNT (*48*) or MWNT (*50*) tips.

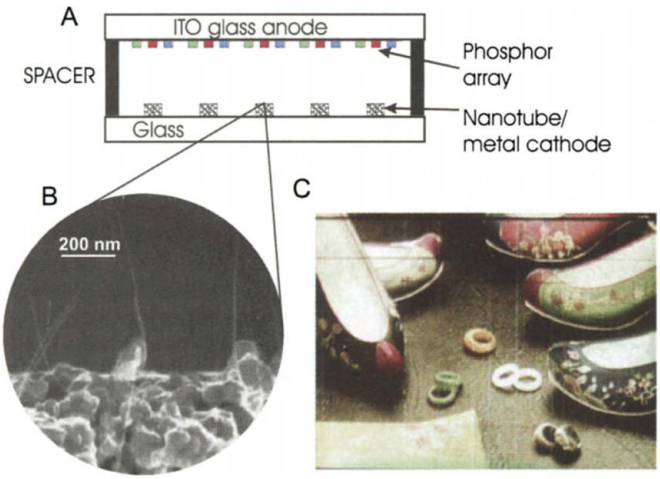

Fig. 2. (**A**) Schematic illustration of a flat panel display based on carbon nanotubes. ITO, indium tin oxide. (**B**) SEM image (*49*) of an electron emitter for a display, showing well-separated SWNT bundles protruding from the supporting metal base. (**C**) Photograph of a 5-inch (13-cm) nanotube field emission display made by Samsung.

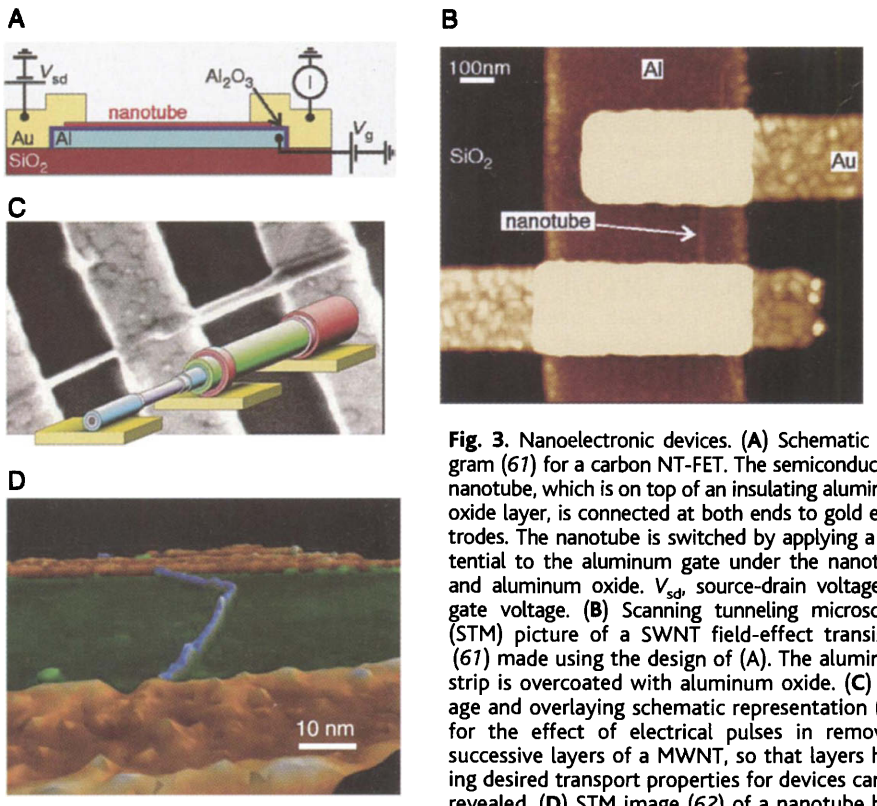

Fig. 3. Nanoelectronic devices. (**A**) Schematic diagram (*61*) for a carbon NT-FET. The semiconducting nanotube, which is on top of an insulating aluminum oxide layer, is connected at both ends to gold electrodes. The nanotube is switched by applying a potential to the aluminum gate under the nanotube and aluminum oxide. V_{sd}, source-drain voltage; V_g, gate voltage. (**B**) Scanning tunneling microscope (STM) picture of a SWNT field-effect transistor (*61*) made using the design of (A). The aluminum strip is overcoated with aluminum oxide. (**C**) Image and overlaying schematic representation (*14*) for the effect of electrical pulses in removing successive layers of a MWNT, so that layers having desired transport properties for devices can be revealed. (**D**) STM image (*62*) of a nanotube having regions of different helicity on opposite sides of a kink, which functions as a diode; one side of the kink is metallic, and the opposite side is semiconducting. The indicated scale bar is approximate.

Nanotube field-emitting surfaces are relatively easy to manufacture by screen-printing nanotube pastes and do not deteriorate in moderate vacuum (10^{-8} torr). These are advantages over tungsten and molybdenum tip arrays, which require a vacuum of 10^{-10} torr and are more difficult to fabricate (*55*). Nanotubes provide stable emission, long lifetimes, and low emission threshold potentials (*47*, *50*). Current densities as high as 4 A/cm^2 have been obtained, compared with the 10 mA/cm^2 needed for flat panel field emission displays and the >0.5 A/cm^2 required for microwave power amplifier tubes (*56*).

Flat panel displays are one of the more lucrative nanotube applications being developed by industry. However, they are also technically the most complex, requiring concurrent advances in electronic addressing circuitry, the development of low-voltage phosphors, methods for maintaining the required vacuum, spacers withstanding the high electric fields, and the elimination of faulty pixels. The advantages of nanotubes over liquid crystal displays are a low power consumption, high brightness, a wide viewing angle, a fast response rate, and a wide operating temperature range. Samsung has produced several generations of prototypes (Fig. 2), including a 9-inch (23-cm) red-blue-green color display that can reproduce moving images (*49*). Despite this impressive development, it is not certain when or whether the flat panel nanotube displays will be commercially available, considering concurrent improvements in relatively low-cost flat panel liquid crystal displays and the emerging organic and polymeric light-emitting diode displays.

Nanotube-based lamps are similar to displays in comprising a nanotube-coated surface opposing a phosphor-coated substrate, but they are less technically challenging and require much less investment. High-performance prototypes seem suitable for early commercialization, having a lifetime of >8000 hours, the high efficiency (for green phosphors) of environmentally problematic mercury-based fluorescent lamps, and the luminance required for large stadium-style displays (*50*). Nanotube-based gas discharge tubes may also soon find commercial use for protecting telecommunications networks

against power surges. Devices comprising nanotube-containing cathodes separated from an anode by a millimeter-wide argon-filled gap provided a 4- to 20-fold improvement in breakdown reliability and an ~30% decrease in breakdown voltage, as compared to commercial devices (*51*).

If a metal target replaces the phosphorescent screen at the anode in a field emission device and the accelerating voltage is increased, x-rays are emitted instead of light. The resulting x-ray source has provided improved quality images of biological samples, probably because the energy range of the impacting electrons is narrower than that for thermionic electron sources (*52*). The compact geometry of nanotube-based x-ray tubes suggests their possible use in x-ray source arrays for medical imaging, possibly even for x-ray endoscopes for medical exploration. Another application requiring intense electron beams is for microwave generation. Here, improving the lifetime of the nanotube emitter under very high current (~500 mA/cm^2) operating conditions is a key technical challenge (*53*).

Nanometer-Sized Electronic Devices

Electronic circuits cannot continue to shrink by orders of magnitude and provide corresponding increases in computational power, unless radically different device materials, architectures, and assembly processes are developed. Dramatic recent advances have fueled speculation that nanotubes will be useful for downsizing circuit dimensions. For example, current-induced electromigration causes conventional metal wire interconnects to fail when the wire diameter becomes too small. The covalently bonded structure of carbon nanotubes militates against similar breakdown of nanotube wires, and because of ballistic transport, the intrinsic resistance of the nanotube should essentially vanish. Experimental results show that metallic SWNTs can carry up to 10^9 A/cm^2, whereas the maximum current densities for normal metals are ~10^5 A/cm^2 (*2*, *57*). Unfortunately, the ballistic current carrying capability is less useful for presently envisioned applications because of necessarily large contact resistances. An electronic circuit involving electrical leads to and from a SWNT will have a resistance of at least $h/4e^2$ or 6.5 kilohms, where h is Planck's constant and e is the charge of an electron (*58*). Contacting all layers in a MWNT could reduce this contact resistance, but it cannot be totally eliminated.

In nanotube field effect transistors (NT-FETs), gating has been achieved by applying a voltage to a submerged gate beneath a SWNT (Fig. 3, A and B), which was contacted at opposite nanotube ends by metal source and drain leads (*59*). The transistors were fabricated by lithographically applying electrodes to nanotubes that were either randomly distributed on a silicon substrate or positioned on the substrate with an atomic force microscope (*60*, *61*).

A transistor assembled in this way may or may not work, depending on whether the chosen nanotube is semiconducting or metallic, over which the operator generally has no control. It is possible to selectively peel outer layers from a MWNT (Fig. 3C) until a nanotube cylinder with the desired electronic properties is obtained (*14*), but this process is not yet very reliable and is probably unsuitable for mass production. Overall device sizes for current NT-FETs, including contacts, are several hundred nanometers, not radically smaller than silicon-based field-effect transistors. A further reduction in size will require, among others, advances in microlithography.

Research toward nanoscopic NT-FETs aims to replace the source-drain channel structure with a nanotube. A more radical approach is to construct entire electronic circuits from interconnected nanotubes. Because the electronic properties depend on helicity, it should be possible to produce a diode, for example, by grafting a metallic nanotube to a semiconducting nanotube. Such a device has been demonstrated. The bihelical nanotube was not, however, rationally produced; rather, it was fortuitously recognized in a normal nanotube sample by its kinked structure (Fig. 3D), which was caused by the helicity change (*62*). The development of rational synthesis routes to multiply branched and interconnected low-defect nanotubes with targeted helicity would be a revolutionary advance for nanoelectronics.

Recent developments have focused considerable media attention on nanotube nanoelectronic applications. With crossed SWNTs, three- and four-terminal electronic devices have been made (*63*), as well as a nonvolatile memory that functions like an electromechanical relay (*64*). Integrated nanotube devices involv-

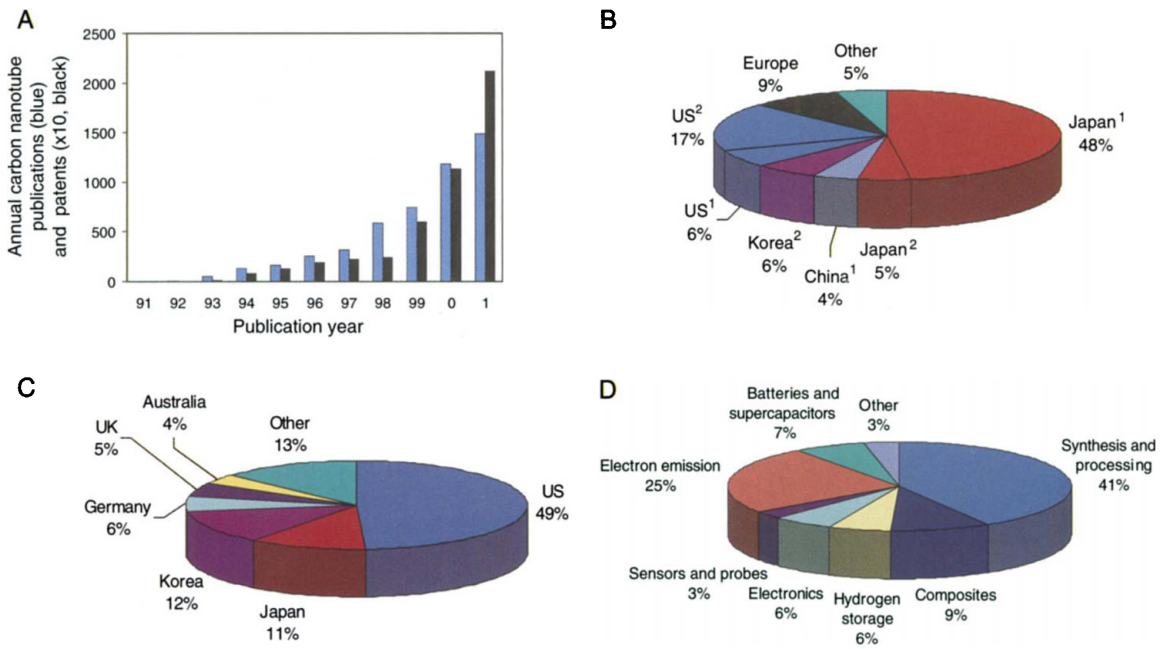

Fig. 4. (**A**) Comparison of the annual number of scientific publications with the number of patent filings and issuances for the carbon nanotube area (*71*). (**B**) Percentages of total patent filings and issuances made by individuals in a country or region and filed either in the same location (superscript 1) or in a different location (superscript 2). (**C**) Percentages of multicountry (world or European) patent filings and issuances that originate from different countries. (**D**) Patent filings and issuances divided according to the main area of the invention. Although the database for these figures is dependent on the search method and involves judgments in assignments, the information shown here is thought to be reliable.

ing two nanotube transistors have been reported (*61*, *64*), providing visions of large-scale integration. Patterned growth of SWNTs on a 4-inch (10-cm) silicon wafer (*65*) may prove an important step toward integrated nanotube electronics. IBM expects that nanotube electronics will be realized in about a decade (*66*). In reaching that goal, formidable technical hurdles must be overcome. Silicon technology is so entrenched that it will take an overwhelmingly compelling new technology to replace it. Nanotubes do not yet qualify, but the potential payoff is so great that this exciting research is amply justified from even a commercial viewpoint.

Sensors and Probes

Possible chemical sensor applications of nonmetallic nanotubes are interesting, because nanotube electronic transport and thermopower (voltages between junctions caused by interjunction temperature differences) are very sensitive to substances that affect the amount of injected charge (*17*, *67*). The main advantages are the minute size of the nanotube sensing element and the correspondingly small amount of material required for a response. Major challenges remain, however, in making devices that differentiate between absorbed species in complex mixtures and provide rapid forward and reverse responses.

Carbon nanotube scanning probe tips for atomic probe microscopes are now sold by Seiko Instruments and manufactured by Daiken Chemical Company, Ltd. The mechanical robustness of the nanotubes and the low buckling force dramatically increase probe life and minimize sample damage during repeated hard crashes into substrates. The cylindrical shape and small tube diameter enable imaging in narrow, deep crevices and improve resolution in comparison to conventional nanoprobes, especially for high sample feature heights (*26*, *68*). Covalently modifying the nanotube tips, such as by adding biologically responsive ligands, enables the mapping of chemical and biological functions (*69*). Nanoscopic tweezers have been made that are driven by the electrostatic interaction between two nanotubes on a probe tip (*70*). They may be used as nanoprobes for assembly. These uses may not have the business impact of other applications, but they increase the value of measurement systems for characterization and manipulation on the nanometer scale.

The Past as Harbinger of the Future

The exponential increase in patent filings and publications on carbon nanotubes indicates growing industrial interest that parallels academic interest (Fig. 4A) (*71*). By percentage of total patent filings (53%), inventors in Japan have led the way (Fig. 4B), but 90% of these patent filings have not yet appeared as filings in other countries. If multicountry foreign filings (world and European patents) are used to gauge the perceived importance of inventions (Fig. 4C), Japan and Korea run a close race, and the United States has a fourfold advantage over each of them.

Consistent with the demonstrated commercial importance of nanotubes in composites, most of the patent filings (50%) are for nanotube synthesis, processing, and composites (Fig. 4D). Reflecting the advanced state of carbon nanotube displays and the attractiveness of related applications, electron emission devices command 25% of the patent filings. Nanotube electronic devices, which might have the most potential for changing the field, provided only 6% of the total patent filings. Impressive advances have been made in demonstrating nanotube electronic device concepts, but a decade or more of additional progress is likely required to reliably assess if and when these breakthroughs will reach commercial application.

Independent of the outcome of the ongoing races to exploit nanotubes in applications, carbon nanotubes have provided possibilities in nanotechnology that were not conceived in the past. Nanotechnologies of the future in many areas will build on the advances that have been made for carbon nanotubes.

References and Notes

1. S. G. Louie, *Top. Appl. Phys.* **80**, 113 (2001).
2. W. Liang *et al.*, *Nature* **411**, 665 (2001).
3. S. P. Frank, P. Poncharal, Z. L. Wang, W. A. de Heer, *Science* **280**, 1744 (1998).
4. P. Kim, L. Shi, A. Majumdar, P. L. McEuen, *Phys. Rev. Lett.* **87**, 215502 (2001).
5. M. Kociak *et al.*, *Phys. Rev. Lett.* **86**, 2416 (2001).
6. Z. K. Tang *et al.*, *Science* **292**, 2462 (2001).
7. G. Gao, T. Çağın, W. A. Goddard, *Nanotechnology* **9**, 184 (1998).
8. M.-F. Yu, B. S. Files, S. Arepalli, R. S. Ruoff, *Phys. Rev. Lett.* **84**, 5552 (2000).
9. D. A. Walters *et al.*, *Appl. Phys. Lett.* **74**, 3803 (1999).
10. E. W. Wong, P. E. Sheehan, C. M. Lieber, *Science* **277**, 1971 (1997).
11. R. G. Ding, G. Q. Lu, Z. F. Yan, M. A. Wilson, *J. Nanosci. Nanotechnol.* **1**, 7 (2001).
12. A listing of commercial suppliers of carbon nanotubes and related materials is available at www.rdg.ac.uk/~scsharip/tubes.htm.
13. P. Ball, *Nature* **414**, 142 (2001).
14. P. G. Collins, M. S. Arnold, Ph. Avouris, *Science* **292**, 706 (2001).
15. H. G. Tennent, U.S. Patent 4,663,230 (5 May 1987).
16. "Mitsui to begin construction of high-volume production plant for carbon nanotubes," www.mitsui.co.jp/tkabz/english/index.html (26 December 2001).
17. P. G. Collins, K. Bradley, M. Ishigami, A. Zettl, *Science* **287**, 1801 (2000).
18. A. Thess *et al.*, *Science* **273**, 483 (1996).
19. A. G. Rinzler *et al.*, *Appl. Phys. A* **67**, 29 (1998).
20. R. H. Baughman *et al.*, unpublished data.
21. R. Haggenmueller, H. H. Gommans, A. G. Rinzler, J. E. Fischer, K. I. Winey, *Chem. Phys. Lett.* **330**, 219 (2000).
22. B. Vigolo *et al.*, *Science* **290**, 1331 (2000).
23. R. H. Baughman, *Science* **290**, 1310 (2000).
24. V. A. Davis *et al.*, in preparation.
25. Z. F. Ren *et al.*, *Science* **282**, 1105 (1998).
26. J. H. Hafner, C. L. Cheung, C. M. Leiber, *Nature* **398**, 761 (1999).
27. S. Fan *et al.*, *Science* **283**, 512 (1999).
28. J. I. Sohn, S. Lee, H. Kim, *Appl. Phys. Lett.* **78**, 901 (2001).
29. Y. Huang, X. Duan, Q. Wei, C. M. Lieber, *Science* **291**, 630 (2001).
30. The Web site of Hyperion Catalysis International, Inc., is available at www.fibrils.com.
31. M. J. Biercuk *et al.*, *Appl. Phys. Lett.* **80**, 2767 (2002).
32. P. Glatkowski *et al.*, U.S. Patent 6,265,466 (24 July 2001).
33. D. Qian, E. C. Dickey, R. Andrews, T. Rantell, *Appl. Phys. Lett.* **76**, 2868 (2000).
34. K. H. An *et al.*, *Adv. Funct. Mater.* **11**, 387 (2001).
35. C. Niu, E. K. Sickel, R. Hoch, D. Moy, H. Tennent, *Appl. Phys. Lett.* **70**, 1480 (1997).
36. C. Niu, J. Kupperschmidt, R. Hock, in *Proceedings of the 39th Power Sources Conference* (Maple Hill, NJ, 2000), pp. 314–317.
37. R. H. Baughman *et al.*, *Science* **284**, 1340 (1999).
38. B. Gao *et al.*, *Chem. Phys. Lett.* **307**, 153 (1999).
39. F. Disma, C. Lenain, B. Beaudoin, L. Aymard, J.-M. Tarascon, *Solid State Ionics* **98**, 145 (1997).
40. M. S. Dresselhaus, K. A. Williams, P. C. Eklund, *Mater. Res. Soc. Bull.* **24**, 45 (2000).
41. G. G. Tibbetts, G. P. Meisner, C. H. Olk, *Carbon* **39**, 2291 (2001).
42. M. Hirscher *et al.*, *J. Alloys Compounds* **330–332**, 654 (2002).
43. C. Zandonella, *Nature* **410**, 734 (2001).
44. Y. Ye *et al.*, *Appl. Phys. Lett.* **74**, 2307 (1999).
45. Y. Chen *et al.*, *Appl. Phys. Lett.* **78**, 2128 (2001).
46. A. C. Dillon, M. J. Heben, *Appl. Phys. A* **72**, 133 (2001).
47. W. A. de Heer, A. Châtelain, D. Ugarte, *Science* **270**, 1179 (1995).
48. A. G. Rinzler *et al.*, *Science* **269**, 1550 (1995).
49. N. S. Lee *et al.*, *Diamond Relat. Materials* **10**, 265 (2001).
50. Y. Saito, S. Uemura, *Carbon* **38**, 169 (2000).
51. R. Rosen *et al.*, *Appl. Phys. Lett.* **76**, 1668 (2000).
52. H. Sugie *et al.*, *Appl. Phys. Lett.* **78**, 2578 (2001).
53. O. Zhou, personal communication.
54. J.-M. Bonard *et al.*, *Phys. Rev. Lett.* **81**, 1441 (1998).
55. J.-L. Kwo *et al.*, *J. Vac. Sci. Technol. B* **19**, 23 (2001).
56. W. Zhu, C. Bower, O. Zhou, G. Kochanski, S. Jin, *Appl. Phys. Lett.* **75**, 873 (1999).
57. Z. Yao, C. L. Kane, C. Dekker, *Phys. Rev. Lett.* **84**, 2941 (2000).
58. Z. Yao, C. Dekker, Ph. Avouris, *Top. Appl. Phys.* **80**, 147 (2001).
59. S. Tans *et al.*, *Nature* **393**, 49 (1998).
60. R. Martel, T. Schmidt, H. R. Shea, T. Hertel, Ph. Avouris, *Appl. Phys. Lett.* **73**, 2447 (1998).
61. A. Bachtold, P. Hadley, T. Nakanishi, C. Dekker, *Science* **294**, 1317 (2001); published online 4 October 2001 (10.1126/science.1065824).
62. Z. Yao, H. Ch. Postma, L. Balents, C. Dekker, *Nature* **402**, 273 (1999).
63. M. S. Fuhrer *et al.*, *Science* **288**, 494 (2000).
64. T. Rueckes *et al.*, *Science* **289**, 94 (2000).
65. N. R. Franklin, Y. Li, R. J. Chen, A. Javey, H. Dai, *Appl. Phys. Lett.* **79**, 4571 (2001).
66. "At IBM, a tinier transistor outperforms its silicon cousins," *New York Times*, 20 May 2002, p. C4.
67. J. Kong *et al.*, *Science* **287**, 622 (2000).
68. H. Dai, J. H. Hafner, A. G. Rinzler, D. T. Colbert, R. E. Smalley, *Nature* **384**, 147 (1996).
69. S. S. Wong, E. Joselevich, A. T. Woolley, C. L. Cheung, C. M. Lieber, *Nature* **394**, 52 (1998).
70. P. Kim, C. M. Lieber, *Science* **286**, 2148 (1999).
71. The analysis of patents and publications used the SciFinder Scholar search system (www.cas.org/SCIFINDER/SCHOLAR/) for the term "carbon nanotube."

72. J. W. G. Wildoer, L. C. Venema, A. G. Rinzler, R. E. Smalley, C. Dekker, *Nature* **391**, 59 (1998).
73. We thank many researchers in the nanotube area for their insights, especially J. E. Fischer, S. Roth, R. Hoch, L. Crosthwait, and J. Robertson. We also thank S. Collins, J. S. Lamba, and S. Lee for their contributions to the figures and the analysis using the SciFinder search system. Supported by Defense Advanced Research Projects Agency contracts N00173-99-2000 and MDA972-02-C-0005.